Roton relaxation in parahydrogen crystals measured by time-resolved stimulated Raman gain

C. Sierens, A. Bouwen, E. Goovaerts, M. De Mazière,* and D. Schoemaker
Physics Department, Universitaire Instelling Antwerpen, B-2610 Wilrijk-Antwerpen, Belgium
(Received 5 August 1987)

Picosecond time-resolved dephasing measurements of the Raman-active $J=2$ rotons in para-H_2 single crystals have been performed with the stimulated-Raman-gain technique. The three distinct $J=2$ rotons ($|M_J|=0$, 1, or 2) could be selected by a proper choice of the polarizations of the four laser beams with respect to the crystal axes. Excellent exponential fits were obtained for the decay curves, indicating little or no inhomogeneous broadening. The resulting T_2 times exhibit no temperature dependence between 5 and 10 K and are in good agreement with recent high-resolution spectral measurements. However, the present time-domain results are more reliable and accurate. In the explored range of ortho-H_2 impurity concentration of up to 5%, a linear increase is found for the relaxational linewidths ($\sim 1/T_2$) with nearly equal slopes for the different $|M_J|$ rotons. These results extrapolated to pure para-H_2 yield T_2 times in the neighborhood of 100 ps which agree quite well with those of a recent microscopic calculation. However, in the experiments unpredicted and significant differences (up to 30%) are evident between T_2 times for different $|M_J|$ values. The rotational relaxation was also measured in the liquid phase of para-H_2 and a value $T_2=7.5$ ps was obtained. It too showed a small decrease with increasing ortho-H_2 concentration.

I. INTRODUCTION

The development of picosecond laser sources has generated considerable experimental and theoretical interest in the coherence decay of excitations in molecular crystals. The decay of vibrational and librational coherence has been measured by coherent anti-Stokes Raman scattering (CARS) in solid N_2,[1] ortho-para mixtures of solid hydrogen,[2] naphthalene,[3-5] and isotopically mixed benzene crystals.[6] The larger molecules possess more vibrational modes, enabling population (T_1) decay to the lower-lying vibrational levels. The influence of isotopic substitution and the temperature dependence demonstrate that T_1 decay really dominates the disappearance of the coherent excitation. These processes yield exponential decays with rather short T_1 lifetimes ranging from the experimental resolution (<5 ps) up to 250 ps.

In the diatomic molecular crystals, however, the coherence decay of the vibrons is attributed to pure T_2 dephasing. One observes considerable longer T_2 decay times, ranging from 1 ns up to 150 ns, and the decay is slower than exponential. The pure dephasing of the A_g vibron in α-N_2 crystals is ascribed to static disorder,[1] leading to T_2 decay curves which depend on the crystal-growing procedure. In this material no influence of isotopic impurities was found. In para-H_2 crystals the dephasing rate of the vibron is strongly enhanced by scattering from ortho-H_2 impurities.[2] The dephasing time of the libron in N_2 was not measured directly, but an upper limit of 72 ps was obtained.[1]

Solid hydrogen is one of the simplest molecular crystals and forms an interesting object for investigations of coherence decay because of the large amount of experimental and theoretical results already available.[7,8] Quantum-mechanical effects in particular have a large influence on the vibrational and rotational properties of these crystals. Hydrogen molecules exist in two species, the stable para-H_2 and the metastable ortho-H_2, possessing a total nuclear spin $I=0$ and 1, respectively. Because of the quantum-mechanical condition of anti-symmetry of the total wave function under permutation of the protons, these molecules can only occur in even- and odd-J rotational states, for para-H_2 and ortho-H_2, respectively. This yields the interesting and exceptional situation that there exist two species which are chemically and isotopically identical, but for which the lowest rotational excitation energies $\Delta E_{\rm rot}$ are very different: $\Delta E_{\rm rot}^{\rm para}=6B$ and $\Delta E_{\rm rot}^{\rm ortho}=10B$ where $B\simeq 59$ cm^{-1} is the rotational constant of the molecule.

Even in solid H_2, the molecules behave as nearly free rotators: They are coupled by anisotropic intermolecular interactions—predominantly the electric quadrupole-quadrupole (EQQ) interaction—which are weak ($\simeq 1$ cm^{-1}) compared to the rotational constant B. The resulting traveling rotational excitations are called rotons. The strong Raman spectrum of the $J=2$ rotons in solid para-H_2 is centered at 355 cm^{-1} and is split by the EQQ interaction into three equidistant lines separated by 2.0 cm^{-1}, which correspond to the $k\simeq 0$ rotons labeled by $|M_J|=1$, 2, and 0 in increasing order of Raman shift. The rotons, although of excitonic nature like the vibrons, possess a number of distinguishing features such as the degeneracy of the $J=2$ rotational level and the particular form of the EQQ interactions which also lead to very different dispersion relations.[9] Moreover, the existence of the ortho-H_2 species yields the opportunity to incorporate in the crystal an impurity which hardly alters the structural properties of the crystal and which possesses very well-known interactions (i.e., the same as for para-H_2) with the host molecules.

Most of the dephasing experiments described in the literature so far have been performed with CARS.[1-6] In

this technique, two coincident laser pulses with a frequency difference $\omega_L - \omega_S$ in resonance with the Raman transition prepare a coherent Raman excitation. The decay of the latter is probed with a progressively delayed replica of the highest frequency ω_L pulse. The interaction of the coherent excitation with the latter creates an anti-Stokes beam $2\omega_L - \omega_S$ in a direction different from the other beams by several degrees, which is determined by phase-matching conditions.

In our experiments we have we have employed the picosecond time-resolved stimulated-Raman-gain (TRSRG) technique (Sec. II B), first proposed by Heritage[10] and whose basis was recently thoroughly reanalyzed.[11,12] The excitation is identical to CARS, but the probing is performed with a delayed identical pulse pair (ω_L, ω_S), crossing the pump beam under a conveniently small angle so as to allow spatial separation of the probe and pump pairs in the subsequent detection scheme. The interaction of the probe pair with what is left of the coherent excitation creates a gain on one beam and a loss on the other beam of the probe pair, and the power change of one of these beams is measured. This signal exceeds the signal obtained by CARS by several orders of magnitude. However, the signal-to-noise ratio does not improve correspondingly as one might be led to expect because of the noise on the laser beam on which the signal is superimposed and the phase noise produced by relative random fluctuating phases of the laser fields. This gain (or loss) signal is still a small part (approximately equal to 10^{-5} in the case of the rotons of para-H_2) of the laser probe beam on which the signal is superimposed. Modulation of the laser beams followed by an appropriate detection scheme[10,13,14] suppresses the noise and yields signal strengths from which dephasing times can be determined with an accuracy comparable to CARS. In evaluating the merits of the TRSRG technique compared to CARS, one should keep in mind that the TRSRG signal decays with a time constant equal to T_2 instead of $T_2/2$ for the corresponding CARS signal. Consequently, our measured decay over almost two orders of magnitude corresponds to almost four orders of magnitude in CARS, which is a typical measuring range reached by the latter (see, e.g., the vibron decay[2] in para-H_2). For further comparison between both techniques we refer to literature.[15–17]

In this paper we present measurements of the dephasing of the coherently excited Raman-active $J=2$ rotons in para-H_2 single crystals with ortho-H_2 concentrations ranging from $c_{\text{ortho}}=0.14\%$ to about 5%. In contrast to the case of the vibrons in para-H_2 the rotons decay exponentially and possess much shorter dephasing times, T_2, with an upper limit in pure para-H_2 crystals of $T_2 \simeq 100$ ps.

A given $|M_J|$ roton mode was selected by judiciously exploiting its polarization properties and by eliminating the beatings in the dephasing signal caused by interference effects between the different modes (Sec. III). The beating patterns also yielded a convenient way to determine the orientation of the grown hexagonal (hcp) H_2 crystal.

The present measurements are compared (Sec. IV) to very recent experiments in the frequency domain by high-resolution spontaneous Raman scattering.[18–20] The results are in overall agreement with each other, but the higher accuracy and reliability of the present time-domain measurements are emphasized. The T_2 times extrapolated to pure para-H_2 are compared to the results of a recent quantum-mechanical calculation.[21] The linear dependence of the inverse T_2 time on ortho-H_2 concentration is discussed in terms of impurity scattering of the $\mathbf{k} \simeq 0$ rotons into the same energy rotons throughout the Brillouin zone, and the differences between roton and vibron scattering are commented on.

II. EXPERIMENTAL

A. Sample preparation and characterization

Hydrogen gas with low ortho-H_2 impurity concentration (0.25%) was obtained by evaporating liquid normal hydrogen in contact with an Apachi nickel silica gel catalyst at 21 K.[8,18,20] Samples of this converted gas were taken at successive days after preparation, which determined the amount of ortho-H_2 due to slow para-H_2 to ortho-H_2 conversion in the glass bulb, in which the gas was stored at room temperature. Such sample was condensed at 15 K in a Pyrex tube inside an optical helium cryostat, in which the crystal was slowly (2 h) grown from the bottom tip upwards.[18,20] In spite of the very slow cooling of this crystal from the melting point to the measuring temperature (8 K) some cracks could not be avoided. Nevertheless, the high quality of single crystals was clear from the beating patterns (see Sec. III) of the dephasing signal which were independent of the interaction region in the crystal. In order to get the purest para-H_2 crystals (0.14% ortho-H_2) a special procedure was employed.[18] The converted H_2 liquid in contact with the Apachi nickel silica gel is boiled off at low pressure just below 18 K and immediately condensated in the Pyrex sample tube at 15 K.

The ortho-H_2 concentration c_{ortho} was determined from the integrated spontaneous Raman intensity I_0 of the $J=1$ to $J=3$ transition of the ortho-H_2, relative to the intensity I_p of the Raman active $J=0$ to $J=2$ transition of para-H_2:[8,20]

$$c_{\text{ortho}} = \frac{rI_0/I_p}{1+rI_0/I_p} ,$$

in which $r=1.73$ is a constant determined by the transition matrix elements between the rotational states, the probability of the occupation of these states, and the Stokes shifted frequencies. The spontaneous Raman spectra were obtained with 100 mW of Ar^+ ion laser light at 514.5 nm. No difference in intensity ratios was obtained when determined both in the liquid and solid states.

B. The time-resolved stimulated Raman gain apparatus

In the TRSRG apparatus (see Fig. 1) the laser pulses with frequencies ω_L and ω_S are generated by two R6G dye lasers (120 mW average output power each) synchronously pumped by a cw mode-locked Ar^+ ion laser with an average output power of 1 W and a repetition frequency of 82 MHz. Each dye laser beam is split into two beams of equal power (BS1 and BS2 in Fig. 1), and the beams with different frequencies are combined (BS3 and BS4) into two collinear (ω_L,ω_S) pairs for pumping and probing, respectively. In the sample the two pairs interact under a conveniently chosen small angle (approximately equal to 5°) so as to permit spatial separation of the pump and probe beams in the subsequent detection scheme. The pump pair creates a coherent excitation when the frequency difference $\omega_L-\omega_S$ is in resonance with a Raman transition of the medium. The probe pair—which can be progressively delayed with respect to the pump pair by a variable delay (VD in Fig. 1)—interrogates the decay of this coherent excitation. This is measured by detecting the Raman gain or loss of one of the laser beams of this probe pair. The power of each of the four dye laser beams in the interaction region ranges between 10 and 20 mW. The pulses of the dye lasers are about 10 ps long. However, the time resolution of TRSRG is determined by a correlation function of the four interacting laser fields, yielding a resolution better than 4 ps,[11,12] which is also distinctly higher than for CARS.

The TRSRG signal is small compared to the intense ω_L or ω_S probe beam on which it is superimposed and is very susceptible to noise from two sources: laser intensity noise and phase noise. The latter is induced by the relative randomly fluctuating laser fields interacting in the sample and originates from the random relative path-length fluctuation of the pump and probe laser pairs caused by slowly wagging mirrors, air turbulence, etc. The double phase modulation technique developed to cope with this[13] was modified in order to improve both

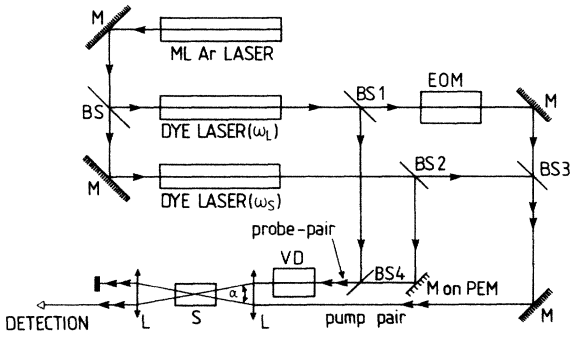

FIG. 1. Schematic representation of the experimental apparatus for time-resolved stimulated Raman gain. The number of arrows in the optical paths indicate the number of collinear beams. (M) mirror, (BS) beam splitter, (L) lens, (EOM) electro-optic modulator, (PEM) piezo-electric modulator, (VD) variable delay, (S) sample.

speed and ease of operation. Laser intensity noise was dealt with by high frequency (10.84 MHz) *intensity* modulation of the ω_L pump beam employing an electro-optical modulator (EOM in Fig. 1) followed by standard lock-in detection.[14] The phase noise and the induced 10.84-MHz pickup noise were eliminated by a low frequency ($\Omega_M=180$ Hz) *phase* modulation—accomplished by a piezo-electrically-driven mirror—of one of the laser beams and by processing the signal (on the ω_S probe beam in our case) by a lock-in amplifier in the ACVM mode, i.e., detecting the squared signal. The rationale for doing this will now be described.

The TRSRG gain or loss signal depends on the product of the electric fields of the laser beams, and as a result it also depends on the relative phase $\Delta\Phi=(\Phi_{L'}-\Phi_{S'})-(\Phi_L-\Phi_S)$ of the beams. $\Phi_{L'}$, $\Phi_{S'}$, Φ_L, and Φ_S are the phases of the ω_L and ω_S beam of the probe and pump field, respectively. The signal is then given by

$$S=S_0\sin\Delta\Phi+N\ . \tag{2.1}$$

S_0 contains the electric fields of the four laser beams, the response of the medium, and the time delay between the pulses and the dephasing time.[10–13,22] N describes the noise from the electric components (lock-in amplifier) and from the laser beam falling on the detecting photodiode. It is assumed that the 10.84-MHz high-frequency demodulation by a lock-in has already occurred when writing down (2.1). In that case S_0 is not modulated. Because of the fluctuating path length changes the relative phase of the two pairs, $\Delta\Phi$ fluctuates, and this was observed to occur on time scale of a few seconds to minutes.[13] These fluctuations can be drastic because a change by π changes the signal to its opposite value.

In the last part of our detection stage the signal (2.1) is squared. We then obtain two phase-dependent terms $\cos2\Delta\Phi$ and $\sin\Delta\Phi$. When the phase fluctuations are rapid and random, these terms are eliminated by a low-pass filter just before the last output, leaving a stable $S_0^2/2$ term—which is proportional to the dephasing signal one wants to measure—superimposed on the dc part of the squared noise background $N_{\rm dc}^2$. This noise term was observed to be very stable and could be subtracted afterwards. Rapid and random phase fluctuations are intrinsic to scanning of the time delay (VD in Fig. 1), due to the vibrations of the optical elements on the variable delay table during such a scan. The relatively high speed (100 ps in less than 1 min) of the variable delay table does not disturb the signal detection in our technique. In fact it is the opposite: A higher speed generates more rapid phase fluctuations, which better eliminate the phase-dependent terms by the low-pass filter. Thus when scanning, a low-frequency phase modulation is not necessary. However, during the alignment of the apparatus the delay table remains stationary. When optimizing the signal one does not know whether the signal increases either due to a slow phase change or a better alignment. Therefore the phase-dependent terms have to be eliminated by the imposed 180-Hz low frequency phase modulation (PEM in Fig. 1). For the modulation function a ramp with a phase amplitude of 2π is taken, yielding a phase

modulation $\Delta\Phi=\Delta\Phi_0+\Omega_M t$, in which $\Delta\Phi_0$ is the former unmodulated slowly varying phase and $\Omega_M t$ is the imposed phase modulation. This modulation function insures that all phase-dependent terms are eliminated by the low-pass filter, in contrast to other modulation functions[13] which may yield unmodulated phase terms in the Fourier expansion of $\cos 2\Delta\Phi$ and $\sin\Delta\Phi$. Although in principle not necessary, we also imposed this phase modulation during a time scan in order to better guarantee the elimination of the phase-dependent terms.

The modulations due to random phase fluctuations or the imposed ramp phase modulation (with amplitude 2π) also solve the problem of the high-frequency pickup. Because the pickup yields a dc or slowly varying disturbing signal at the output of the high-frequency lock-in amplifier, it is blocked by a dc filter at the input of the ACVM before squaring. The TRSRG signal is transmitted by this filter because it fluctuates or is modulated.

The wavelength of one of the dye lasers and the time delay between the pump and probe pulses, generated by a variable optical path length (VD in Fig. 1), are set and scanned by steppermotors and controlled by a personal computer (PC), which also registers the data during a scan. The employed double modulation and demodulation technique in conjunction with PC steering permit quick scans and data registration. A full decay curve can be recorded in less than 5 min. This high speed is indispensable for the large number of scans needed during the limited time (~ 7 h) before the H_2 crystal is completely sublimated and condensed at a colder point in the Pyrex tube.

First, many tens of scans with different orientations of the crystal and different polarizations and wavelengths of the laser beams had to be taken in order to determine the hexagonal axis of the crystal. After this procedure, the T_2 decays of the three $|M_J|$ peaks were measured, and this was done repeatedly in order to check the reproducibility of the decay times in the same and in different parts of the crystal and, through averaging, to improve the signal-to-noise ratio.

III. POLARIZATION PROPERTIES AND ROTON SELECTION

We succeeded in determining the orientation of the hexagonal axis of the crystal—which we further on will call the z axis—from the observed beating pattern of the T_2 decay. The mutually perpendicular x and y axes are arbitrarily chosen in the plane perpendicular to the z axis. The measured dephasing signals (see Fig. 2) for different combinations of the polarizations of the laser beams clearly show beating patterns[11,22] with periods of 8.3 and 16.7 ps. These correspond to the frequency differences of 4 cm^{-1} between the two outmost roton peaks and 2 cm^{-1} between neighboring peaks, respectively. Due to the low combined spectral resolution [full width at half maximum (FWHM$\approx$8 cm^{-1})] of both dye lasers the $|M_J|$ peaks could not be selected separately by wavelength tuning. They are excited simultaneously. Their Raman tensors differ, however, and the $|M_J|$ peaks can therefore, in principle, be separately detected by distinct linear polarization combinations of the four 2×2 collinear laser beams.

Stimulated Raman scattering is a nonlinear process of third order in the electric fields **E**. The nonlinear response of a medium is described by the third-order polarization field $P_i^{(3)}$ (Refs. 15–17, 22):

$$P_i^{(3)}=\chi_{ijkl}^{(3)}E_jE_kE_l\ , \tag{3.1}$$

in which $\chi_{ijkl}^{(3)}$ is the third-order susceptibility of the medium and E_m $(m=j,k,l)$ is the total electric field. $ijkl$ represent Cartesian indices, and the summation convention is assumed. In our experiment the total electric field consists of the sum of the electric fields of the four interacting laser beams. Then according to (3.1) the polarization field contains different contributions corresponding to two-photon absorption, third-harmonic generation, stimulated Raman scattering, etc.[15–17,22] The part of $\chi_{ijkl}^{(3)}$ describing the stimulated Raman process $\chi_{ijkl}^{(3)R}$ can be related to the Raman tensor α of spontaneous Raman scattering[15–17,22]

$$\chi_{ijkl}^{(3)R}\sim\langle a\,|\,\alpha_{ij}\,|\,b\rangle\langle b\,|\,\alpha_{kl}\,|\,a\rangle\ , \tag{3.2}$$

with $|a\rangle$ and $|b\rangle$ the initial and final states. In our experimental apparatus (see Fig. 1) only the Raman part is measured. All the other contributions are eliminated because of (i) the frequency at which the signal is detected, (ii) the geometrical configuration yielding phase mismatches for various other contributions, and (iii) the double modulation and demodulation technique.[13] However, at zero time delay between pump and probe pulses there remain, in principle, some nonresonant, orientational, and two-photon absorption and instantaneous Raman contributions, which disappear with increasing time delay, and only the main Raman contribution remains.[11] In para-H_2 it appears that these contributions are very small since no peak is observed at zero time delay (see Figs. 2 and 3). So the measured signal is determined by the Raman part (3.2), and the polarization properties are then obtained from this expression, and the spontaneous Raman tensors α presented in Table I.

The $|M_J|=0$ peak is selected with $zzzz$ (corresponding to the above-mentioned Cartesian indices) polarizations [see Fig. 2(a)], in which the first two letters refer to the polarization directions of the high- (ω_L) and low- (ω_S) frequency laser beams of the probe pair, respectively, and the last two to the polarization directions of the corresponding beams of the pump pair. From (3.2) and Table I it can readily be derived that the other modes do not contribute. Similarly, the $|M_J|=1$ and $|M_J|=2$ peaks are selected by $zxzx$ [see Fig. 2(f)] and $yxyx$ polarizations, respectively. Because the laser beams propagate horizontally, the latter is only possible if the crystal is grown with the hexagonal axis horizontal, something we cannot control. Therefore the $|M_J|=2$ dephasing time is not measured in all of the experiments, and consequently fewer points are plotted in Fig. 4 for this roton.

The selection of a single roton transition by a given polarization combination is perfect only if the polarizations of the laser fields are completely along the indicated principal axes of the crystal. However, this requirement is

not exactly met in the experiment because the orientation of the hexagonal axis of a crystal can only be determined within a certain albeit narrow range and because of the slight elliptical character of the polarizations of the laser beams. This explains the remaining beatings in Figs. 1(b), 1(c), and 1(e), since part of the decay connected with the other $|M_J|$ rotons is detected. However, the interference of the other modes can be strongly suppressed by setting the frequency difference $\Delta\nu$ between the maxima of the spectral distributions of the dye lasers into resonance with the $|M_J|$ roton one wants to observe [Figs. 2(a),2(f)]. The frequency difference $\Delta\nu$ is not accurately defined because of the broad (5 cm^{-1}) spectral laser lines. However, small changes of $\Delta\nu$ with respect to the laser linewidth clearly do have an effect, as is evident from the strength of the beating in the various figures in Fig. 2.

One can analyze the contributions from unwanted rotons for small deviations of the polarizations with respect to the above-mentioned configurations. For example, the $M_J=0$ roton is selected by the *zzzz* configuration, and small-angle deviations yield contributions of the $|M_J|=2$ roton only to fourth order in this angle, while the $|M_J|=1$ contribute to second order. This can be deduced from expression (3.2) and Table I. As a result only a 8.3-ps beating between the $|M_J|=0$ and 1 rotons shows up in this polarization geometry, and it becomes clearly suppressed when $\Delta\nu$ is increased [Figs. 2(a)–(c)]. In the *zxzx* geometry, which selects the $|M_J|=1$ roton, both the $|M_J|=0$ and 2 rotons are contributing to second order in the deviation angles, and as a result both 8.3-ps and 16.7-ps periods appear in the beating patterns [Fig. 2(e)].

The orientation of the crystal is determined from the beating pattern obtained with all polarizations mutually

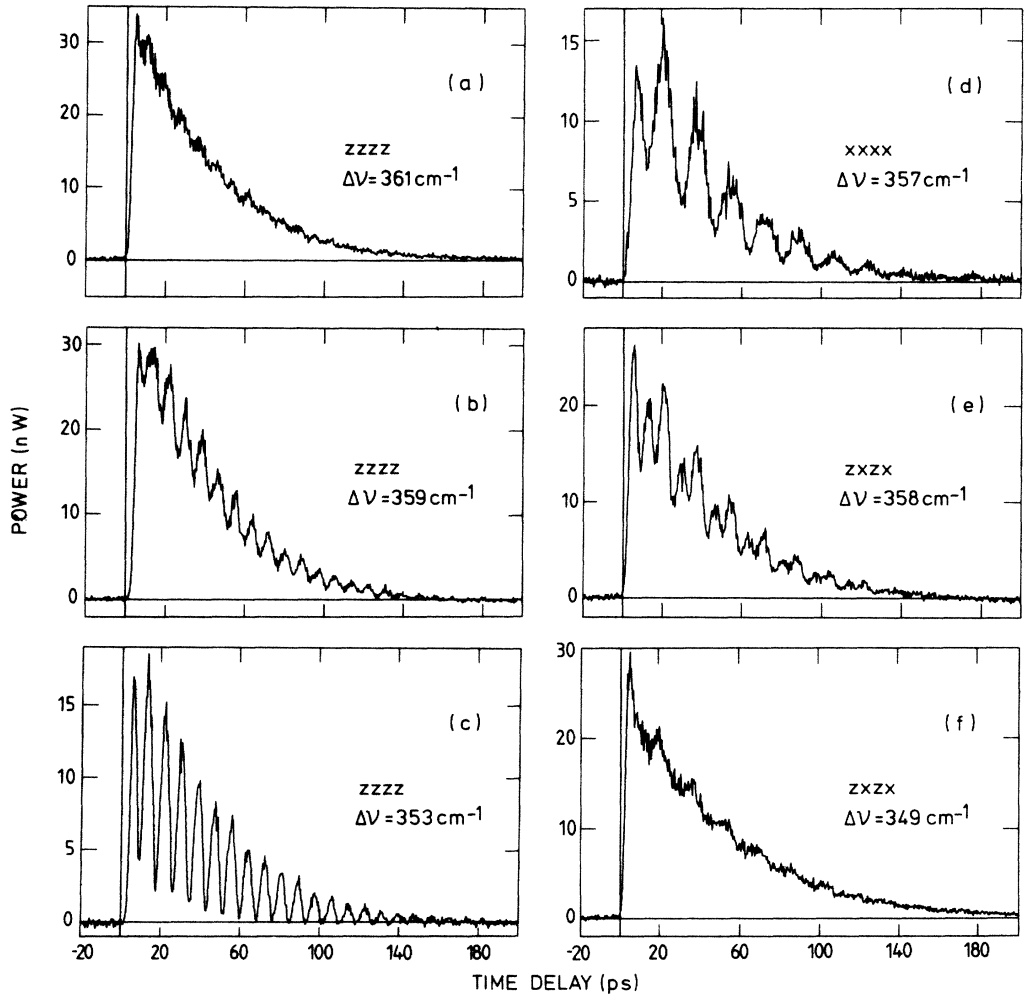

FIG. 2. Recorded time-resolved stimulated Raman gain signal (background subtracted) for different polarizations (*zzzz*,*xxxx*,*zxzx*) and wave-number differences $\Delta\nu$ between the two dye lasers. From such spectra the orientation of the crystal can be determined and checked. The ortho-H_2 concentration is 0.36% except for (d) where $c_{ortho}=0.26\%$. The figures with the same polarization geometry are put above each other in order of increasing $\Delta\nu$. This clearly illustrates that the best selection of the single roton transition [$|M_J|=0$ in (a), $|M_J|=1$ in (f)] occurs for the outer edge of the roton Raman spectrum.

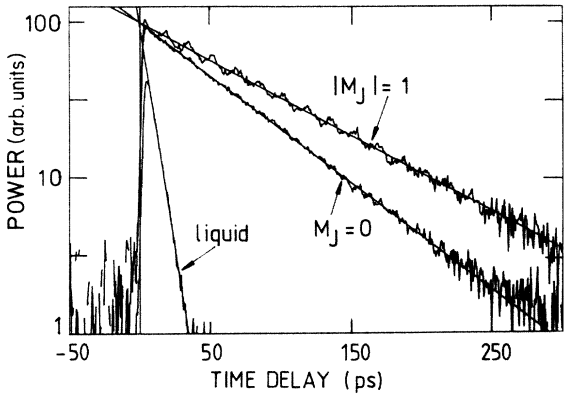

FIG. 3. Exponential fits presented on a semilogarithmic plot of the roton decays $M_J=0$ ($T_2=63\pm2$ ps) and $|M_J|=1$ ($T_2=89\pm3$ ps) in solid H_2, and the rotational excitation decay in liquid H_2 ($T_2=7.5\pm1.0$ ps) obtained with *zzzz*, *zxzx*, and *zzzz* polarizations, respectively (0.14% ortho-H_2). The measurements were performed at $T=8$ K in the solid and at $T=15$ K in the liquid.

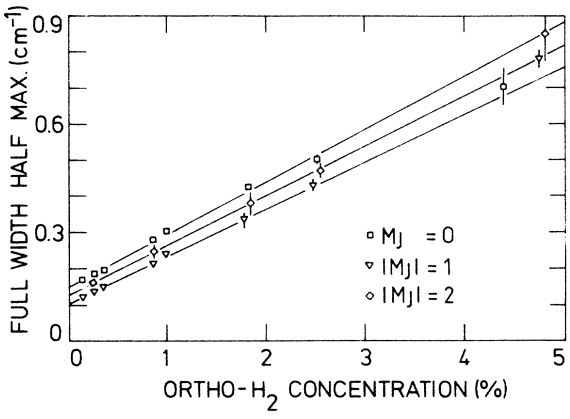

FIG. 4. Linear dependence on the ortho-H_2 concentration of the linewidth (FWHM) $\delta\nu=1/\pi T_2$ of the Raman modes, determined from the measured T_2 times.

parallel, by minimization of this pattern while rotating the sample tube around a vertical axis and the polarizations around the beam propagation direction. Only when the polarizations are close to the z axis such that the $|M_J|=2$ mode contribution is reduced to fourth order does the 16.7-ps beating period disappear. This, therefore, is a good indication that the polarizations of the four beams are close to the z axis, and with minor polarization and orientation adjustments the remaining beating can be eliminated. As a check other polarization geometries can subsequently be measured, e.g., the *xxxx* geometry employed in Fig. 2(d), in which the expected strong 16.7-ps beating is observed.

IV. RESULTS CONCERNING ROTON DEPHASING AND DISCUSSION

The dephasing of the $J=2$ rotons in para-H_2 crystals has been measured by TRSRG in crystals with ortho-H_2 concentrations ranging from $c_{\text{ortho}}=0.14\%$ to about 5% (Figs. 2–4). The decay curves for $|M_J|=0$ and 1 rotons are shown in Fig. 3 for the purest para-H_2 sample. From this exponential fit it is seen that, within experimental accuracy, no deviation from exponential behavior can be observed. As pointed out before, the decay over two orders of magnitude in TRSRG is equivalent to four orders in time-resolved CARS measurements, which underlines the quality of the exponential fits.

An exponential decay is found at all investigated ortho-H_2 concentrations, and the relaxational linewidth (FWHM) $\delta\nu=1/\pi T_2$ corresponding to the measured T_2 time is plotted as a function of c_{ortho} in Fig. 4. As shown in this figure, the linewidth increases linearly with concentration. The T_2 times for pure para-H_2—obtained by linear interpolation—and the slopes of the linewidths as a function of c_{ortho} are listed in Table II. The dephasing times were checked to be temperature independent between $T\approx5$ K and 10 K. The reproducibility of the results was investigated for different positions in a given crystal, as well as for crystals grown on different occasions. This reproducibility can also be judged from the small scattering of the data points in Fig. 4.

In Fig. 3 we also show for comparison the decay of the coherent $J=2$ rotational excitation in liquid para-H_2 at 15 K. The T_2 times are here much shorter ($T_2=7.5\pm1.0$ ps at $c_{\text{ortho}}=0.14\%$) and depend also somewhat on the ortho-H_2 impurity concentration ($T_2=6\pm1$ ps at

TABLE I. Rotational matrix elements $\langle 2M_J\,|\,\alpha_{ij}\,|\,00\rangle$ of the polarizability tensor of an H_2 molecule (Ref. 7) in which γ is the anisotropic part of the polarizability. From these matrix elements one readily determines the polarization directions of the laser fields which have to be employed in order to select just one roton mode, and these directions are shown in the last row.

$M_J=0$	$M_J=\pm1$	$M_J=\pm2$
$\frac{\gamma}{\sqrt{45}}\begin{bmatrix}-1&0&0\\0&-1&0\\0&0&2\end{bmatrix}$	$\frac{\gamma}{\sqrt{30}}\begin{bmatrix}0&0&\mp1\\0&0&i\\\mp1&i&0\end{bmatrix}$	$\frac{\gamma}{\sqrt{30}}\begin{bmatrix}1&\mp i&0\\\mp i&-1&0\\0&0&0\end{bmatrix}$
zzzz	*zxzx*	*yxyx*

TABLE II. The T_2 dephasing times (in picoseconds) are given of the Raman active rotons in pure para-H_2 crystals ($T=8$ K), (a) from extrapolation to $c_{ortho}=0\%$ of our time-resolved stimulated-Raman-gain measurements (TRSRG), (b) from previous very-high-resolution Raman linewidth experiments (HRRL) (Refs. 18–20), and (c) from a microscopic quantum mechanical calculation (Ref. 21 and comment). The T_2 time of the $J=2$ rotational excitations in liquid para-H_2 ($c_{ortho}=0.14\%$ and $T=15$ K) is also included. (d) The slopes of the linewidth of the $J=2$ roton transitions vs ortho-H_2 concentrations is given as the increase (in cm^{-1}) per percent impurity concentration (see also Fig. 4).

	$M=0$	$\lvert M_J\rvert=1$	$\lvert M_J\rvert=2$	Liquid
(a) TRSRG	71±5	102±7	81±9	7.5±1.0
(b) HRRL	98±9	171±16	125±9	
(c) Theory	89	95	92	
(d) Slope	0.15±0.01	0.13±0.01	0.14±0.01	

$c_{ortho}=5\%$). The previously obtained linewidth in spontaneous Raman scattering[23] of 1.4 cm^{-1} shows that the relation $\delta\nu=1/\pi T_2$ is well satisfied. These linewidth measurements also showed a dependence on the ortho-H_2 concentration ($\delta\nu=3.5$ cm^{-1} in normal H_2). These shorter times are due to the brief, random, and sudden encounters of molecules in the liquid[24,25] instead of the time-independent interactions (EQQ interaction in the roton case) in the solid state.[1] The exponential decay points to the random character of the phase disruptions. Further on, we will always refer to the solid state.

The results of our time-domain experiments are in good overall agreement with recent high-resolution spectral Raman measurements.[18–20] However, the TRSRG measurements have permitted to show that, even at the lowest c_{ortho}—and, by extrapolation, also for pure para-H_2—the roton decay is indeed exponential. In this region our time resolution (<4 ps) is much shorter than the decay times (approximately equal to 100 ps). At low c_{ortho} the corresponding linewidths are comparable to the resolution of the spectral measurements (approximately equal to 0.1 cm^{-1}) and therefore the Lorentzian line shape could not be unambiguously demonstrated.[18–20] Moreover, the delicate procedure of deconvolution of the instrumental profile out of the measured spectrum has probably led to an underestimation of the linewidths, and consequently to a systematic overestimation (by up to 65%) of the T_2 times for pure para-H_2 (see Table II). Also at higher c_{ortho} the present measurements are more accurate, as can be seen from comparison of Fig. 4 with the corresponding Fig. 2 of Ref. 18.

The T_2 times determined for pure para-H_2 are in close agreement with those obtained from a recent microscopic calculation[21] (see Table II) taking into account only the EQQ interaction between the molecules, and including single as well as multiple $J=2$ excitations. In this calculation an exponential decay was also predicted. The differences in measured T_2 times for different $\lvert M_J\rvert$ values (up to 30%) are not explained by this theory to the order to which it was carried out. In order to certify that in our experiments the residual linewidth of the $J=2$ rotons in pure para-H_2 is not due to the HD isotopic impurity (natural abundance $c_{HD}=0.03\%$), experiments are now being performed on intentionally HD-doped crystals. Possible influence of low-frequency phonons on the roton lifetimes can be eliminated because of the absence of temperature dependence of the relaxation rate. Higher-order photon-roton interactions with optical phonons ($\Omega_{opt}\approx 120$ cm^{-1}) cannot be excluded on the basis of this observation.

The linear dependence of the Raman linewidth $\delta\nu$ (approximately $1/T_2$) on the ortho-H_2 concentration observed earlier in the frequency domain experiments[18–20] is confirmed with high accuracy by our time-domain experiments (see Fig. 4). The strength of the effect of these impurities may be judged from the fact that 1% of ortho-H_2 contributes to the dephasing rate with the same magnitude as the intrinsic dephasing process in pure para-H_2. The linear increase may be interpreted as though the ortho-H_2 impurities act as quasi-isolated scattering centers which scatter the Raman-active rotons at $\mathbf{k}\approx\mathbf{0}$ into rotons with the same energy at $\mathbf{k}$ vectors throughout the Brillouin zone. Scattering occurs because the impurities in the crystal break the translational symmetry and therefore states with a definite wave vector are not eigenstates. As a result, the initially created coherent state with definite wave vector $\mathbf{k}=\mathbf{0}$—which can be described by a minimum uncertainty superposition of all occupation states accessible by the applied radiation field—then decays. One can look upon this from another point of view. Because of the lack of translational symmetry the $\mathbf{k}=\mathbf{0}$ state is composed of a narrow distribution of energy eigenstates.[1] The energy spread of this distribution will cause the amplitude of the coherent excited state to decay. Impurity scattering in crystals and its influence on the T_2 time has been dealt with for excitonic states in molecular crystals.[26]

It is interesting to compare our results to previous measurements of the decay of vibrational coherence in ortho-para mixtures of solid hydrogen.[2] There too a dependence of the decay time on the ortho-H_2 concentration has been found. However, a slower-than-exponential decay was observed and attributed to the zero density of vibron states at the energy of the $\mathbf{k}=\mathbf{0}$ state (bottom of vibron band). In this case, Fermi's golden rule would predict no decay at all. In contrast, the $\mathbf{k}=\mathbf{0}$ roton states are in the middle of the roton band, at an energy with a finite density of roton states,[9] which explains why our ob-

served roton decays are exponential. The faster decay times of the rotons are not so surprising. In order to get decay times of the same order for the vibron, the zero density of states of the latter should have been compensated by larger transition matrix elements for elastic impurity scattering. However, even in the pure H_2 crystal, where the dephasing is not dominated by elastic impurity scattering, the roton decays are much faster than the vibron decay. Similar to the vibron decay in para-H_2, the A_g vibron in α-N_2 crystals possesses a slower-than-exponential decay because of the zero density of states at the $\mathbf{k}\simeq 0$ A_g vibron energy at the bottom of the vibron band.[1] The pure dephasing, however, results from scattering from static disorder and is independent of isotopic impurities. In view of the experimental observations discussed here and of the underlying theory, we would predict an exponential decay for the $\mathbf{k}\simeq 0$ T_g vibron in α-N_2 because it is located in the middle of the vibron band at a point of high density of states. Both the T_g vibron and the libron dephasing remain to be measured in α-N_2 crystals.

We want to draw attention to the fact that the slope of the dependence of $1/T_2$ on the ortho-H_2 concentration is nearly the same for the three different $J=2$ rotons (see Fig. 4 and Table II). The scattering rate in the golden-rule approximation is determined by matrix elements describing the transition from the $\mathbf{k}=0$ to $\mathbf{k}\neq 0$ states with the same energy, and by the roton density of states at this energy. There seems to be no reason why these transition elements and the density of states should be equal for different $|M_J|$ values. A scattering model calculation, based on a simplified picture for the interaction of the rotons with the ortho-H_2 impurity, is being performed, and preliminary results are in good order of magnitude agreement with the experimental values.[20] Also in this respect the experiments involving a different type of impurity, the HD molecule, could be helpful.

We believe that the influence of possible strain in the crystal on the measured T_2 times are negligible. When cooling down the crystal from the melting point (14 K) to the measuring temperature (8 K) the crystal shrinks substantially. The crystal then loosens with difficulty from the Pyrex tube and cracks appear. These cracks are not homogeneously distributed in the crystal. Nevertheless, the measured T_2 times at different positions in the crystal were still the same. Also, the same T_2 times were measured when new crystals were grown with the same ortho-H_2 concentration.

V. CONCLUSION

Our study of the roton dephasing in para-H_2 has shown that the time-resolved stimulated Raman gain technique[10–12] provides an excellent alternative to time-resolved CARS. The T_2 times of the three distinct $J=2$ rotons corresponding to the different $|M_J|$ values could be directly and more accurately measured than in the previous very high-resolution spontaneous Raman linewidth measurements.[18–20] The magnitudes of the T_2 times in pure para-H_2 are also in good agreement with the result of a recent microscopic calculation.[21] The measured differences between the dephasing times of the three rotons in the pure crystal and the linear dependence of $1/T_2$ as a function of the ortho-H_2 impurity concentration and with nearly the same slope for the different $|M_J|$ values need further investigation.[20]

We also compared our roton results with those on vibrons in para-H_2. Although in both cases the scattering of the $\mathbf{k}=0$ excitons from the ortho-H_2 impurities into $\mathbf{k}\neq 0$ excitons yields an important contribution to the T_2 dephasing, the rotons all decay exponentially, while the vibron decay is slower than exponential. This can be understood from the corresponding nonzero and zero density of state of these excitons.

ACKNOWLEDGMENTS

This work was supported by the Geconcerteerde Acties (Ministerie van Wetenschapsbeleid) and the IIKW (Interuniversitair Instituut voor Kernwetenschappen), to which the authors are greatly indebted. Two of us, E.G. and M. De M., want to thank the NFWO (Nationaal Fonds voor Wetenschappelijk Onderzoek) for financial support.

*Present address: Natuurkundig Laboratorium, Universiteit van Amsterdam, The Netherlands.

[1] I. I. Abram, R. M. Hochstrasser, J. E. Kohl, M. G. Semack, and D. White, J. Chem. Phys. **71**, 153 (1979).

[2] I. I. Abram, R. M. Hochstrasser, J. E. Kohl, M. G. Semack, and D. White, Chem. Phys. Lett. **71**, 405 (1980).

[3] B. H. Hesp and D. A. Wiersma, Chem. Phys. Lett. **75**, 423 (1980).

[4] K. Duppen, B. M. M. Hesp, and D. A. Wiersma, Chem. Phys. Lett. **79**, 399 (1981).

[5] D. D. Dlott, C. L. Schlosser, and E. L. Chronister, Chem. Phys. Lett. **90**, 386 (1982).

[6] F. Ho, W.-S. Tsay, J. Trout, S. Velsko, and R. M. Hochstrasser, Chem. Phys. Lett. **97**, 141 (1983).

[7] J. Van Kranendonk, *Solid Hydrogen* (Plenum, New York, 1983).

[8] I. F. Silvera, Rev. Mod. Phys. **52**, 393 (1980).

[9] A. Lagendijk and I. F. Silvera, Phys. Lett. **84A**, 28 (1981). The roton density of states for hcp para-H_2 crystals were kindly made available to us by A. Lagendijk.

[10] J. P. Heritage, Appl. Phys. Lett. **34**, 470 (1979).

[11] M. De Mazière, Ph.D. thesis, University of Antwerpen, 1986; M. De Mazière C. Sierens, and D. Schoemaker (unpublished).

[12] M. van Exter and A. Lagendijk, Opt. Commun. **56**, 191 (1985).

[13] M. De Mazière and D. Schoemaker, J. Appl. Phys. **58**, 1439 (1985).

[14] B. F. Levine and C. G. Bethea, IEEE J. Quantum. Electron. **QE-16**, 85 (1980).

[15] M. D. Levenson, *Introduction to Nonlinear Laser Spectroscopy* (Academic, New York, 1982).

[16] A. B. Harvey, *Chemical Applications of Nonlinear Raman Spectroscopy* (Academic, New York, 1981).

[17]G. L. Eesley, *Coherent Raman Spectroscopy* (Pergamon, Oxford, 1981).

[18]E. Goovaerts, X.-Y. Chen, A. Bouwen, and D. Schoemaker, Phys. Rev. Lett. **57**, 479 (1986).

[19]E. Goovaerts, X.-Y. Chen, C. Sierens, A. Bouwen, and D. Schoemaker, in *Quantum Aspects of Molecular Motions in Solids*, edited by A. Heidemann, A. Magerl, M. Prager, D. Richter, and T. Springer (Springer-Verlag, Berlin, 1987), p. 217; D. Schoemaker, C. Sierens, A. Bouwen, and E. Goovaerts, Bull. Am. Phys. Soc. **32**, 395 (1987).

[20]X.-Y. Chen, Ph.D. thesis, University of Antwerpen, 1987.

[21]M. Vanhimbeeck, H. De Raedt, A. Lagendijk, and D. Schoemaker, Phys. Rev. B **33**, 4264 (1986). A unit conversion error arising from confusion of the spectroscopic $\tilde{\lambda}=1/\lambda$ with the wave-vector dimension $k=2\pi/\lambda$ has resulted in this paper in T_2 values overestimated by a factor 2π.

[22]A. Penzkofer, A. Laubereau, and W. Kaiser, Prog. Quant. Electron. **6**, 55 (1979).

[23]S. S. Bathnagar, E. J. Allin, and H. L. Welsh, Can. J. Phys. **40**, 9 (1962).

[24]R. Loudon, *The Quantum Theory of Light* (Clarendon, Oxford, 1981).

[25]S. F. Fischer and A. Laubereau, Chem. Phys. Lett. **35**, 6 (1975).

[26]S. Velsko and R. M. Hochstrasser, J. Chem. Phys. **82**, 2180 (1985).